Communication

Resonance Raman Imaging of the NADPH Oxidase Subunit Cytochrome *b*$_{558}$ in Single Neutrophilic Granulocytes

Henk-Jan van Manen, Natallia Uzunbajakava, Robin van Bruggen, Dirk Roos, and Cees Otto

J. Am. Chem. Soc., **2003**, 125 (40), 12112-12113• DOI: 10.1021/ja036973r • Publication Date (Web): 16 September 2003

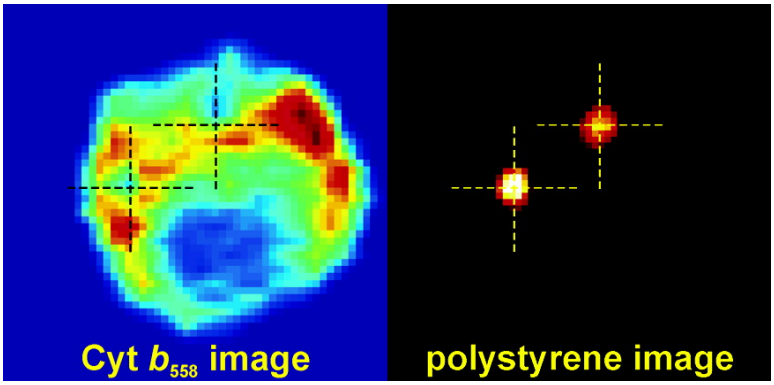

More About This Article

Additional resources and features associated with this article are available within the HTML version:

- Supporting Information
- Links to the 3 articles that cite this article, as of the time of this article download
- Access to high resolution figures
- Links to articles and content related to this article
- Copyright permission to reproduce figures and/or text from this article

View the Full Text HTML

J|A|C|S
COMMUNICATIONS

Published on Web 09/16/2003

Resonance Raman Imaging of the NADPH Oxidase Subunit Cytochrome b_{558} in Single Neutrophilic Granulocytes

Henk-Jan van Manen,*,† Natallia Uzunbajakava,† Robin van Bruggen,‡ Dirk Roos,‡ and Cees Otto†

Department of Science & Technology, Biophysical Engineering Group, University of Twente, P.O. Box 217, 7500 AE Enschede, The Netherlands, and Department of Experimental Immunohematology, Sanquin Research, and Landsteiner Laboratory, Academic Medical Centre, University of Amsterdam, Plesmanlaan 125, 1066 CX Amsterdam, The Netherlands

Received June 30, 2003; E-mail: h.w.j.vanmanen@tnw.utwente.nl

As professional phagocytes, neutrophilic granulocytes are critical in innate immunity because they form the first line of defense against invading microorganisms.[1] Upon ingestion of pathogens, the neutrophils expose the intruders to an array of microbicidal small molecules and proteins. Among these are reactive oxygen species (ROS), which are derived from the superoxide (O_2^-) that is produced from oxygen by the intricate enzyme system NADPH oxidase.[2] It is currently accepted that the catalytic core of NADPH oxidase resides in cytochrome b_{558} (cyt b_{558}), a heterodimeric membrane protein consisting of gp91^{phox} and p22^{phox}. The large glycosylated subunit gp91^{phox} is a flavohemoprotein that contains all of the catalytically active parts. Electron flow from NADPH to oxygen occurs via a bound FAD and two hemes that are embedded in transmembrane helices.

Due to the presence of heme groups, the characterization of cyt b_{558} from neutrophils has been facilitated by resonance Raman (RR) spectroscopy.[3] For example, by comparison with synthetic models of known constitution, Hurst et al. demonstrated that the heme iron centers in cyt b_{558} are low-spin six-coordinate in both ferric and ferrous oxidation states.[4] In our group, we have studied the activation of NADPH oxidase by both soluble and particulate activators by recording high-quality RR spectra from the cytoplasm of living neutrophils on a home-built confocal Raman microscope.[5,6] Upon activation, a (partial) reduction of the cyt b_{558} hemes occurs, which is reflected in a significant shift of the ν_4 oxidation-state marker band[7] from 1375 to 1362 cm^{-1} in the RR spectrum.

We here demonstrate that the subcellular distribution of cyt b_{558} in single neutrophils can be visualized by scanning over a cell while gathering RR spectra. Moreover, we show that part of the cyt b_{558} pool translocates from the membranes of specific granules (which contain ~80−90% of the cyt b_{558} in resting neutrophils)[8] to particle-containing phagosomes upon stimulating the cells with serum-coated polystyrene (PS) beads. The presence of cyt b_{558} in isolated phagocytic vacuoles was already shown in 1978 by Segal and Jones.[9] Translocation of cyt b_{558} is necessary for the NADPH oxidase system to release microbicidal ROS only in the phagosome. Previous studies on translocation of cyt b_{558} upon activation have mainly relied on immunocytochemistry combined with electron[10] and fluorescence microscopy[11] and on in vitro marker assays after subcellular fractionation.[8,12] In contrast, our Raman microscopic technique is a label-free, chemical (vibrational) imaging method that can be performed on single, intact cells.

We employed a confocal Raman microscope that was similar to a recently described Raman setup.[13,14] Previously, we used 647 nm excitation light for nonresonant Raman imaging of the subcellular distribution of proteins in lymphocytes and eye lens epithelial cells,[13] and of the distribution of DNA and protein in apoptotic HeLa cells.[14] In the work described here, the 413 nm line from a krypton ion laser (Coherent Innova 90-K) was used for resonant excitation of cyt b_{558} in neutrophils. The laser beam was focused by a 63× water-immersion objective (NA = 1.2) onto the sample, and the Rayleigh and Raman scattered emission was collected through the same objective, passed through a holographic notch filter to suppress Rayleigh scattering, and focused on a pinhole (25 μm diameter) which was positioned at the entrance of a polychromator. A diffraction grating was used to disperse the Raman signal onto a LN-cooled CCD camera.

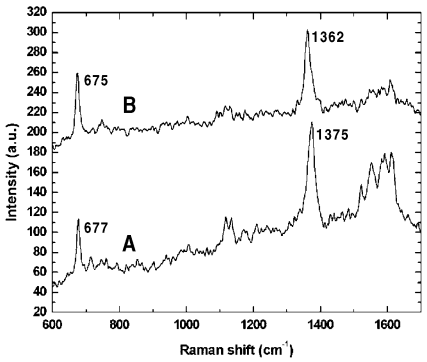

Figure 1. Resonance Raman spectra from the cytoplasm of single neutrophils. Conditions: 1 mW excitation power at 413 nm, 298 K, 10 s accumulation time, 7.5 × 7.5 μm^2 area scanned during signal accumulation (1 s/scan). Spectrum A, fixed neutrophil; spectrum B, dithionite-reduced fixed neutrophil.

Samples for Raman imaging were made by adhering freshly isolated granulocytes (~10^6 cells/mL in PBS/BSA/citrate) onto poly-L-lysine-coated CaF_2 disks, followed by incubation for 15 min at 37 °C with PS beads (1.0 μm diameter) that had been opsonized for 1.5 h with fresh human serum. Phagocytosis and (intra)cellular movement was arrested by fixing the cells in 2% paraformaldehyde for 20 min. For Raman experiments on resting cells, the phagocytosis procedure was omitted.

Typical resonant Raman spectra from the cytoplasm of single neutrophils are shown in Figure 1. When a cytoplasmic area is scanned over, high-quality spectra are obtained with a relatively short accumulation time of 10 s. Upon reduction with dithionite, the diagnostic shift from 1375 (Figure 1A) to 1362 cm^{-1} (Figure 1B) in the iron oxidation-state marker band of the cyt b_{558} hemes is clearly observed.

Raman images were recorded by first positioning a neutrophil in the laser focus using a videocamera and white-light illumination (focus ~2 μm above the substrate), followed by scanning over the cell and accumulating a full RR spectrum at each pixel (typically 1 s/pixel). Data analysis consisted of singular value decomposition

† University of Twente.
‡ University of Amsterdam.

10.1021/ja036973r CCC: $25.00

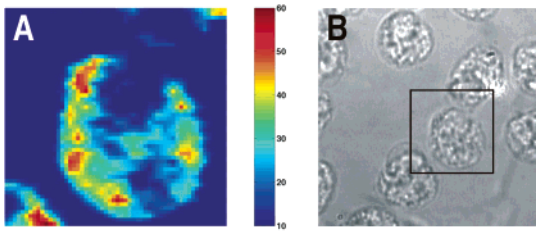

Figure 2. (A) RR image (14×14 μm^2) of a resting neutrophil in the cyt b_{558} band around 1375 cm^{-1}. Conditions: 1 mW excitation power at 413 nm, 298 K, 1 s accumulation time/pixel. (B) Corresponding white-light transmission image. The area enclosed by the black square was used for RR imaging.

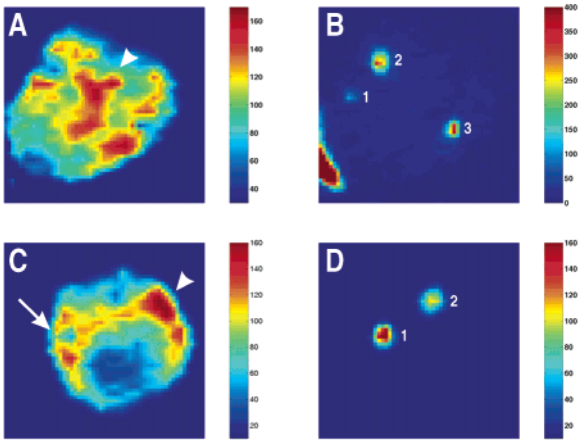

Figure 3. RR images (15×15 μm^2) of the cyt b_{558} (A and C; image in 1362 cm^{-1} band) and PS (B and D; image in 1004 cm^{-1} band) distribution in neutrophils that have phagocytosed PS particles. Conditions are as in Figure 2. The red area in the lower left part of B originates from an uningested cluster of PS beads that was attached to the cell.

(SVD)[15] on the constructed spectral matrix to significantly reduce the noise in the RR spectra.[14] All RR images were constructed by plotting the intensity of the 1375 cm^{-1} band of cyt b_{558} (or 1362 cm^{-1} band in the case of the reduced species), as a function of position. Background signal, likely due to neutrophil flavoprotein autofluorescence,[16] was subtracted.

Figure 2 shows a RR image of the distribution of oxidized cytochrome b_{558} in a fixed neutrophil in the resting state. The multilobed character of the nucleus can be clearly discerned as the region of low intensity. Individual specific granules cannot be visualized because they are small (<0.5 μm diameter), numerous, and therefore probably close together, and the resolution of our imaging technique is limited in this case by the 0.5 μm step size.[17] However, cytoplasmic regions with high cyt b_{558} content are easily recognized (red to yellow regions in Figure 2A).

We next attempted to visualize the spatial redistribution of cyt b_{558} that occurs in neutrophils upon phagocytosis of particles.[8,11] We chose to stimulate neutrophils with serum-coated polystyrene beads because the intense PS Raman scattering would enable us to construct images of these as well (using the same recorded dataset).

Figure 3 shows RR images of neutrophils that have phagocytosed several PS particles. The cells displayed in Figure 3A and C have three and two ingested particles, respectively, which are not in the same focal plane (as observed from the corresponding white-light transmission images, not shown). This is reflected by different intensities in the Raman images of the particles (Figure 3B and D) and verifies the confocal properties of our setup (depth resolution (fwhm) of 2.9 μm). Comparison between the cyt b_{558} and PS images in Figure 3A and B shows that the cyt b_{558} concentration is enhanced in the vicinity of the ingested PS particles. Experiments on other cells show a similar pattern, that is, high cyt b_{558} concentrations near ingested particles. The surrounding pattern as observed in the left part of Figure 3C (see arrow) is not always evident. Because phagocytosis was not synchronized, the starting point for particle uptake and hence cyt b_{558} translocation toward the phagosome is expected to be different for almost every cell and also within one cell. This is exemplified by Figure 3A and C, where it is also seen that a fraction of cyt b_{558} (see arrowheads) is not translocated to the phagosome.

RR spectra from phagosomal areas such as in Figure 3C (arrow) show the presence of both cyt b_{558} (bands at 675 and 1362 cm^{-1}) and PS (e.g., band at 1004 cm^{-1}) in the same femtoliter volume element defined by the confocal microscope, providing proof that phagosomal cyt b_{558} is spatially close to the ingested particle.

The RR microscopy results in this contribution demonstrate the feasibility of label-free, vibrational imaging of enzymatic processes in single neutrophils. The spatial reorganization of cyt b_{558} upon particle phagocytosis can be visualized in these cells. Our results may provide the basis for studies on similar NADPH oxidases found in a number of other cell types[18] and implicated in, for example, cell signaling.

Acknowledgment. Financial support from The CGD Research Trust is gratefully acknowledged. We thank Yvonne Kraan for the isolation of granulocytes from venous blood.

References

(1) (a) Babior, B. M. *Am. J. Med.* **2000**, *109*, 33−44. (b) Burg, N. D.; Pillinger, M. H. *Clin. Immunol.* **2000**, *99*, 7−17.
(2) Vignais, P. V. *Cell. Mol. Life Sci.* **2002**, *59*, 1428−1459.
(3) Tu, A. T. *Raman Spectroscopy in Biology: Principles and Applications*; John Wiley & Sons: New York, 1982; Chapter 12.
(4) Hurst, J. K.; Loehr, T. M.; Curnutte, J. T.; Rosen, H. *J. Biol. Chem.* **1991**, *266*, 1627−1634.
(5) Otto, C.; Sijtsema, N. M.; Greve, J. *Eur. Biophys. J.* **1998**, *27*, 582−589.
(6) Sijtsema, N. M.; Tibbe, A. G. J.; Segers-Nolten, G. M. J.; Verhoeven, A. J.; Weening R. S.; Greve, J.; Otto, C. *Biophys. J.* **2000**, *78*, 2606−2613.
(7) Spiro, T. G. *Resonance Raman Spectra of Heme and Metalloproteins*; Wiley: New York, 1987.
(8) Borregaard, N.; Heiple, J. M.; Simons, E. R.; Clark, R. A. *J. Cell Biol.* **1983**, *97*, 52−61.
(9) Segal, A. W.; Jones, O. T. G. *Nature* **1978**, *276*, 515−517.
(10) (a) Jesaitis, A. J.; Buescher, E. S.; Harrison, D.; Quinn, M. T.; Parkos, C. A.; Livesey, S.; Linner, J. *J. Clin. Invest.* **1991**, *85*, 821−835. (b) Ginsel, L. A.; Onderwater, J. J. M.; Fransen, J. A. M.; Verhoeven, A. J.; Roos, D. *Blood* **1990**, *76*, 2105−2116.
(11) For some examples, see: (a) DeLeo, F. R.; Allen, L.-A. H.; Apicella, M.; Nauseef, W. M. *J. Immunol.* **1999**, *163*, 6732−6740. (b) Johansson, A.; Jesaitis, A. J.; Lundqvist, H.; Magnusson, K.-E.; Sjölin, C.; Karlsson, A.; Dahlgren, C. *Cell. Immunol.* **1995**, *161*, 61−71.
(12) Clark, R. A.; Leidal, K. G.; Pearson, D. W.; Nauseef, W. M. *J. Biol. Chem.* **1987**, *262*, 4065−4074
(13) Uzunbajakava, N.; Lenferink, A.; Kraan, Y.; Willekens, B.; Vrensen, G.; Greve, J.; Otto, C. *Biopolymers (Biospectroscopy)* **2003**, *72*, 1−9.
(14) Uzunbajakava, N.; Lenferink, A.; Kraan, Y.; Volokhina, E.; Vrensen, G.; Greve, J.; Otto, C. *Biophys. J.* **2003**, *84*, 3968−3981.
(15) (a) Golub, G. H.; Van Loan, C, F. *Matrix Computations*; North Oxford Academic Publishing: Oxford, 1983. (b) Henry, E. R.; Hofrichter, J. *Methods Enzymol.* **1992**, *210*, 129−192.
(16) Borregaard, N.; Tauber, A. I. *J. Biol. Chem.* **1984**, *259*, 47−52.
(17) The lateral resolution of our setup is 0.33 μm (fwhm) at 413 nm.
(18) For an overview, see: Lambeth, J. D. *Curr. Opin. Hematol.* **2002**, *9*, 11−17.

JA036973R